Development 133, 2617-2625 (2006) doi:10.1242/dev.02436

calderón encodes an organic cation transporter of the major facilitator superfamily required for cell growth and proliferation of *Drosophila* tissues

Héctor Herranz[1,2], Ginés Morata[2] and Marco Milán[1,*]

The adaptation of growth in response to dietary changes is essential for the normal development of all organisms. The insulin receptor (InR) signalling pathway controls growth and metabolism in response to nutrient availability. The elements of this pathway have been described, although little is known about the downstream elements regulated by this cascade. We identified *calderón*, a gene that encodes a protein with highest homology with organic cation transporters of the major facilitator superfamily, as a new transcriptional target of the InR pathway. These transporters are believed to function mainly in the uptake of sugars, as well as other organic metabolites. Genetic experiments demonstrate that *calderón* is required cell autonomously and downstream of the InR pathway for normal growth and proliferation of larval tissues. Our results indicate that growth of imaginal cells may be modulated by two distinct, but coordinated, nutrient-sensing mechanisms: one cell-autonomous and the other humoral.

KEY WORDS: Insulin pathway, Growth, Wing, *Drosophila*

INTRODUCTION

One of the most obvious differences between animals, even in the same systematic group, e.g. mammals, is size. However, little is known about the mechanisms that underlie the control of cell, organ or body size. The dimensions of an organ and an organism depend on the number of cells and on the size of each individual cell. In multicellular organisms, growth regulation depends on the integration of various genetic and environmental cues (Conlon and Raff, 1999; Stern and Emlen, 1999). Nutrient availability is one of the major environmental signals that affects growth and, as such, complex humoral responses ensure that growth and development are properly coordinated with nutritional conditions.

Multicellular organisms respond to nutrient availability through cell-autonomous and -non-autonomous mechanisms. Growth regulation through the latter occurs via the release of insulin-related growth factors from peripheral tissues. In *Drosophila*, ablation of several neurosecretory cells expressing insulin-like peptides causes a growth defect (Rulifson et al., 2002), and mice lacking an anterior pituitary expressing growth hormone are dwarves (Butler and Le Roith, 2001). Studies in *Drosophila* have highlighted a crucial role for the insulin receptor (InR) pathway in regulating the cell-autonomous response to nutrient availability (reviewed by Goberdhan and Wilson, 2003; Stocker and Hafen, 2000). The InR, a tyrosine kinase transmembrane receptor, induces phosphorylation of insulin receptor substrates (IRS), which activate a cascade of downstream effectors. In vertebrates, genetic manipulation of several elements of this pathway modulates tissue growth *in vivo* thus demonstrating that the insulin-like growth factor (IGF) pathway is required for growth (Efstratiadis, 1998; Shioi et al., 2000; Shioi et al., 2002).

[1]Icrea and Institut de Recerca Biomedica, Parc Cientific de Barcelona, Josep Samitier, 1-5, 08028 Barcelona, Spain. [2]Centro de Biología Molecular 'Severo Ochoa'-CSIC, Campus de Cantoblanco, 28049 Madrid, Spain.

*Author for correspondence (e-mail: mmilan@pcb.ub.es)

Accepted 9 May 2006

The InR downstream effectors PI3 kinase/Dp110 and target of rapamycin (TOR) exert some of their growth effects at the transcriptional level (reviewed by Neufeld, 2003). In yeast, TOR controls the expression of a broad group of genes that are involved in protein, lipid and nucleic acid metabolism (Beck and Hall, 1999; Cardenas et al., 1999). However, in multicellular organisms little is known about effectors of the InR pathway that are regulated transcriptionally. Here we identify *calderón* (*cald*; *orct2* – FlyBase), which encodes an organic cation transporter of the major facilitator superfamily, as a downstream effector of the InR pathway in *Drosophila*. Loss of *cald* activity mimics the phenotype of mutations in the InR pathway during embryonic and adult development. Expression of *calderón* is positively regulated by the InR downstream effectors PI3 kinase/Dp110 and TOR, and its activity is required for TOR-mediated growth induction. Thus, *calderón* is a target of the PI3 kinase/TOR branch of the InR pathway required cell autonomously for insulin-mediated cell growth.

MATERIALS AND METHODS

Drosophila strains

Ultrabithorax-Gal4 (*Ubx-Gal4* in the text; M. Calleja and G. Morata, unpublished), *engrailed-Gal4* (*en-Gal4* in the text) (Tabata et al., 1995), *patched-Gal4* (*ptc-Gal4* in the text) (Wilder and Perrimon, 1995), *MS-1096-Gal4* (Milan et al., 1998), *Kruppel-Gal4* (*Kr-Gal4* in the text) (Castelli-Gair et al., 1994), *EP1072* (Bloomington Stock Centre), *UAS-p35* (Hay et al., 1995), *UAS-Rheb* (a gift from Bruce Edgar) (Saucedo et al., 2003), *UAS-dS6K* (a gift from T. P. Neufeld), *UAS-PI3K92E-Dp110^{D954A}* (a gift from P. Léopold) (Leevers et al., 1996), and *brk^{M12}-lacZ* (Jazwinska et al., 1999) were used. *H(PDelta2-3)HoP2.1* transposase and *UAS-GFP* are described in Flybase. The *UAS-cald* transgenic lines were generated by cloning the whole open reading frame [ORF (isolated by PCR of genomic fly DNA)] into the pUAST vector, using the *Bgl*II/*Xho*I cloning sites. The constructs were injected into *y w^{1118}* embryos, and stable lines were selected by rescue of the *white* phenotype. To distinguish hemizygous or homozygous mutant embryos from their heterozygous siblings, we used the balancer *TM6b, AbdA-lacZ.*

Molecular localization of *calderón-Gal4* and P-element mutagenesis

Using plasmid rescue, we cloned and sequenced the flanking genomic sequence 3′ of the PGawB element (Brand and Perrimon, 1993). The insert is located 422 bp upstream of the CG13610 transcription start. For the generation of P-element excisions, males homozygous for the pGal4 insertion (*Cald-Gal4*) were crossed with females carrying the *H(PDelta2-3)HoP2.1* transposase on the CyO balancer chromosome. Excisions of the PGal4 transposon were selected by the loss of the w^+ eye in the F1 progeny. Individual revertants were crossed with TM3/TM6B flies and balanced. PCR analysis was performed with individual stocks corresponding to a new complementation group. We used one primer located 480 bp downstream of the P-element insertion site and another primer located 330 bp upstream of this site: downstream primer: 5′-GTCTGTCTGTCGC-AGCGCAGC-3′; upstream primer: 5′-GCAACTGACTTCGTCGA-GTGGCGCCGG-3′.

The mutants recovered corresponded to new insertions of 2.7 Kb (R106), 9 Kb (R107) and 50 bp (R161) in the same place, 11 bp downstream of the original LP1 insertion site.

Analysis of the *calderón^{R161}* developmental delay

Embryos that were 0-24 h old were collected, and the development of heterozygous *cald^{R161}/+ and* homozygous *cald^{R161}* animals was analyzed. 77 heterozygous *cald^{R161}/+* larvae required 5-6 days to reach the pupal stage and 5 days to eclose as adults. Ten homozygous *cald^{R161}* larvae required 8-9 days to reach the pupal stage and 6 days to eclose as adults. Homozygous *cald^{R161}* individuals were identified by the absence of the Humeral dominant marker of the *TM6b* balancer chromosome.

Genetic mosaics

The following *Drosophila* strains were used to generate loss-of-function clones: *FRT82B cald^{R107}/TM6B; FRT82B cald^{R106}/TM6B; FRT82B cald^{R161}/TM6B; FRT82B cald^{EP1072}/TM6B; hs-FLP122; FRT82B arm-lacZ; hs-FLP122; FRT82B ubiGFP; ywhs-FLP122; FRT82B arm-lacZ y$^+$ M(3R); yhs-FLP122 tub-Gal4:UAS-GFP; FRTR82B tub-Gal80*.

The FLP/FRT technique (Xu and Rubin, 1993) was used to generate loss-of-function clones. Larvae of the appropriate genotypes were heat shocked for 1 h at 37°C, at different larval stages. The clones were visualized in discs by either loss of GFP or β-Gal expression.

Immunostaining of embryos and discs

Discs were dissected in PBS and fixed in 4% paraformaldehyde for 20 min at room temperature. They were subsequently washed in PBS, blocked in blocking buffer (PBS, 0.3% Triton, 1% BSA), and incubated overnight with the primary antibody diluted in blocking buffer at 4°C. Washes were performed in blocking buffer, and the appropriate fluorescent secondary antibody was added for 1 h at room temperature. Following further washes in blocking buffer, the discs were mounted in Vectashield. Anti-FOXO antibody was kindly provided by Oscar Puig, anti-β-Gal (rabbit) and anti-caspase 3 were purchased from Cappel and from Cell Signalling, respectively. Images were taken in a laser MicroRadiance microscope (Bio-Rad) and subsequently processed using Adobe Photoshop. In situ hybridization was performed as described in (Azpiazu and Frasch, 1993), and embryos were mounted in Permount (Fisher Scientific). *cald* antisense Digoxigenin-labelled RNA probes were generated as described in (Tautz and Pfeifle, 1989) using the EST SD08136 (Berkeley *Drosophila* Genome Project).

Preparation of larval and adult cuticles

Adult flies were prepared by the standard methods for microscopic inspection. Soft parts were digested with 10% KOH, washed with alcohol and mounted in Euparal. Embryos were collected overnight and aged an additional 12 h. First instar larvae were dechorionated in commercial bleach for 3 min and the vitelline membrane was removed using heptano-methanol 1:1. After washes with 100% methanol and 0.1% Triton X-100, larvae were mounted in Hoyer's lactic acid (1:1) and allowed to clear at 65°C for at least 24 h.

RESULTS AND DISCUSSION

calderón encodes an organic cation transporter expressed in embryonic and imaginal tissues

The *LP1-Gal4* line was found in an enhancer trap screen performed in the adult fly (Calleja et al., 1996; Herranz and Morata, 2001). We selected this line for further analysis on the basis of its expression pattern in the developing embryo (see below). The insertion is located on the right arm of chromosome 3 polytene section 95F8, 422 bp upstream of the transcription start site of *CG13610* (Fig. 1A). We analyzed *CG13610* expression during embryonic and imaginal disc development. The expression pattern found in *LP1-Gal4; UAS-lacZ* embryos and imaginal discs was similar to that of *CG13610,* as visualized by in situ hybridization (Fig. 1). From now onwards we refer to *CG13610* as *calderón* (*cald*) and *LP1-Gal4* as *cald-Gal4*.

cald started to be expressed ubiquitously at the cellular blastoderm stage (Fig. 1C). At germ band extended stage, *cald* transcripts were found in a broad region of the dorsal side (Fig. 1F). As development proceeded, *cald* expression was restricted to amnioserosa cells and the central nervous system (Fig. 1B,G,H; a transverse section of the embryo at this stage showed an expression pattern that resembled the shape of a 'calderón', the Spanish name for the music symbol that increases the length of a music note).

cald was ubiquitously expressed in the eye, leg, wing and haltere discs, although with regional modulation (Fig. 1I-N); its expression was stronger in the pouch region of the wing (Fig. 1I,J) and in the region posterior to the morphogenetic furrow in the eye (Fig. 1K,L). The antennal disc showed two rings of higher *cald* expression (Fig. 1K,L), while expression in the leg disc was greater in the distal domain (Fig. 1M,N).

CG13610 has been mapped cytologically to 95F8, encodes a 567-amino-acid-protein with 11 transmembrane domains, with highest homology with organic cation transporters of the major facilitator superfamily. Genes identified as putative homologs have been identified in *Homo sapiens*, *M. musculus* and *G. Gallus*, among others (Fig. 1O and data not shown). Mutations in the human homolog *slc22a4* cause rheumatoid arthritis (Tokuhiro et al., 2003) and Crohn's disease (Peltekova et al., 2004), probably because of defects in the transport of organic metabolites.

Embryonic and imaginal requirement of *calderón*

The original *cald-Gal4* insertion is viable without any overt phenotype. To perform a functional analysis of *cald*, we induced mutations by mobilization of the P-element. We isolated three embryonic lethal alleles (*cald^{R106}*, *cald^{R107}*, *cald^{R165}*) and one homozygous viable allele (*cald^{R161}*). Sequence analysis revealed that *cald^{R106}* and *cald^{R107}* bear truncated P-elements of 2.7 and 9 Kb, respectively, but 11 bp further downstream from the *cald-Gal4* original insertion site. *cald^{R161}* has a P-element fragment of only 50 bp located at the same insertion point as the two previous lethal alleles. We were unable to characterize the *cald^{R165}* allele. The lethal alleles *cald^{R165}*, *cald^{R106}* and *cald^{R107}* greatly reduce *CG13610* mRNA expression (compare Fig. 2E with F, and data not shown). Another independent P-element insertion, *EP1072*, located further upstream of the original *cald-Gal4* insertion, is embryonic lethal, strongly reduces the levels of *CG13610* mRNA expression and drives the expression of *calderón* in a GAL4-dependent way (Fig. 2G,H and data not shown). Embryos homozygous for the *cald^{EP1072}*, *cald^{R165}*, *cald^{R106}* and *cald^{R107}* mutations showed the characteristic U-shape phenotype of embryos unable to retract the germ band, probably because of abnormal development of the amnioserosa [compare Fig. 2B,C with 2A (Frank and Rushlow, 1996)]. Embryo-mutants for *InR* present the same phenotype (Fig. 7F) (Fernandez et al., 1995).

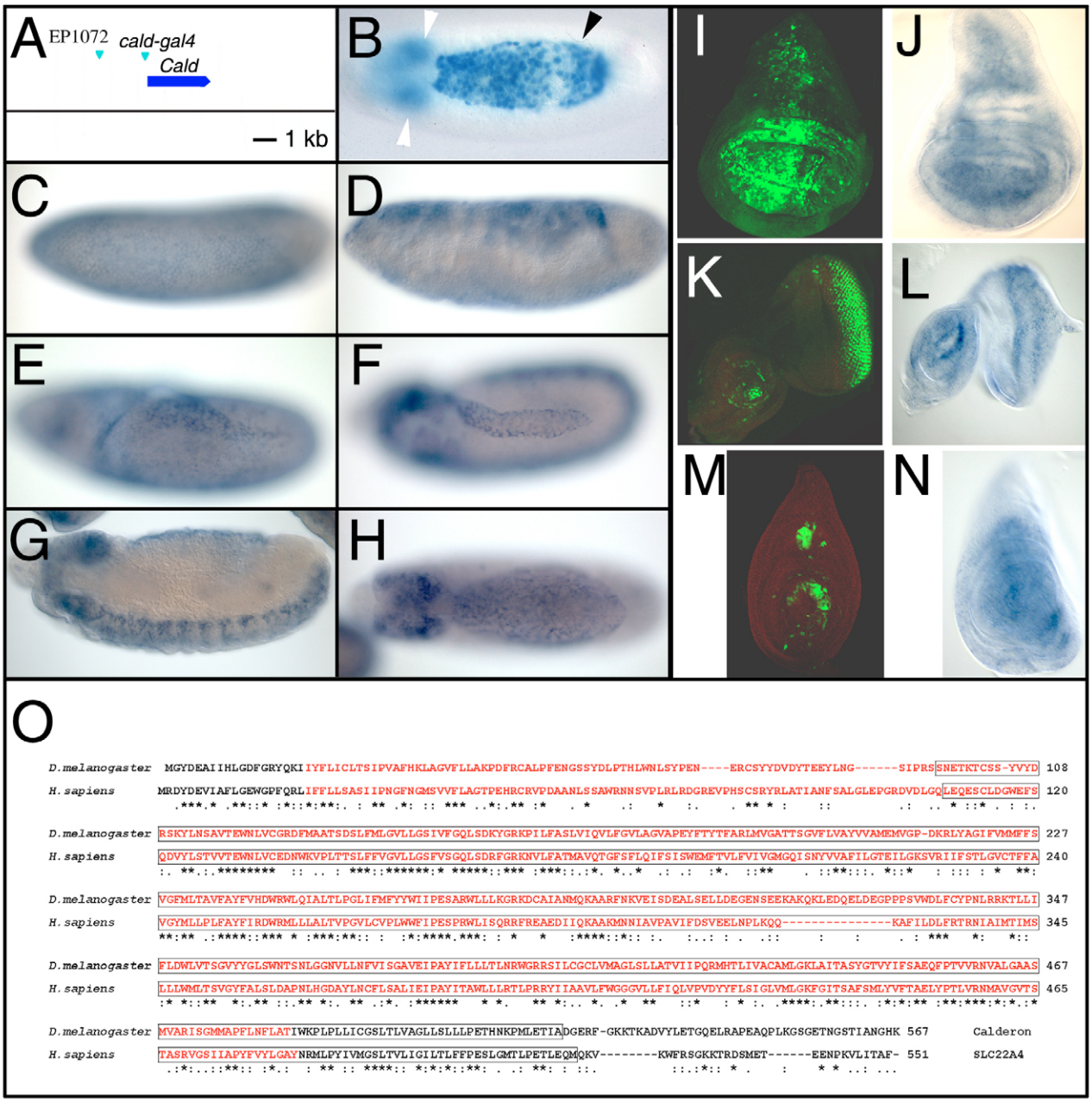

Fig. 1. *calderón* expression in embryonic and imaginal tissues. (**A**) Genomic organization of the *cald* locus. The P-element insertions *cald-gal4* and *EP1072* are shown as blue triangles. (**B**) Dorsal view of a *cald-Gal4; UAS-lacZ* embryo at stage 13. Note *lacZ* expression, visualized by histochemical staining for β-gal activity, in the amnioserosa (black arrowhead) and in the central nervous system (CNS, white arrowhead). (**C-G**) Lateral view (anterior left, dorsal up) of embryos showing the distribution of *CG13610* transcripts from stage 5 (C) to 13 (G). Early embryos (C) have uniform levels of *cald* expression. Gastrula embryos (D) have higher levels of *cald* transcripts in the most dorsal cells. From germ band extended (E,F) to germ band retracted embryos (G). *cald* expression is restricted to the amnioserosa and the CNS. (**H**) Dorsal view of an embryo at stage 13 showing *cald* expression in the amnioserosa and the CNS, which reproduces *cald-Gal4* expression (compare with B). (**I**,**K**,**M**) *cald-Gal4:UAS-GFP* staining in wing (I), eye-antenna (K) and leg (M) imaginal discs. (**J**,**L**,**N**) Wing (J), eye-antenna (L) and leg (N) imaginal discs showing *cald* transcripts. *cald* transcripts reproduce the *cald-Gal4* expression. (**O**) Alignment of Calderon and the human protein SLC22A4. Both proteins have 11 transmembrane domains with a Major Facilitator Superfamily domain (boxed amino acids) and a Sugar Transporter domain (red amino acids). Identical amino acids are identified by a star. Double dots label conserved substitutions and single dots semi-conserved substitutions. The two proteins are 36.4% identical.

Development of flies homozygous for the viable allele $cald^{R161}$ was markedly delayed during larval and pupal development (Fig. 3A). Adult flies were smaller than wild-type animals (fly length ratio of *calderón*/wild-type animals was 0.9±0.04; Fig. 3B,E). Mutant wings and eyes were also smaller (eye size ratio of *calderón*/wild-type animals was 0.8±0.05; wing size ratio of *calderón*/wild-type animals was 0.85±0.04; Fig. 3C-E). Cell density was increased in the absence of *cald* activity, indicating that cell size but not cell number was affected (wing cell density ratio of *calderón*/wild-type animals was 1.3±0.16; Fig. 3E).

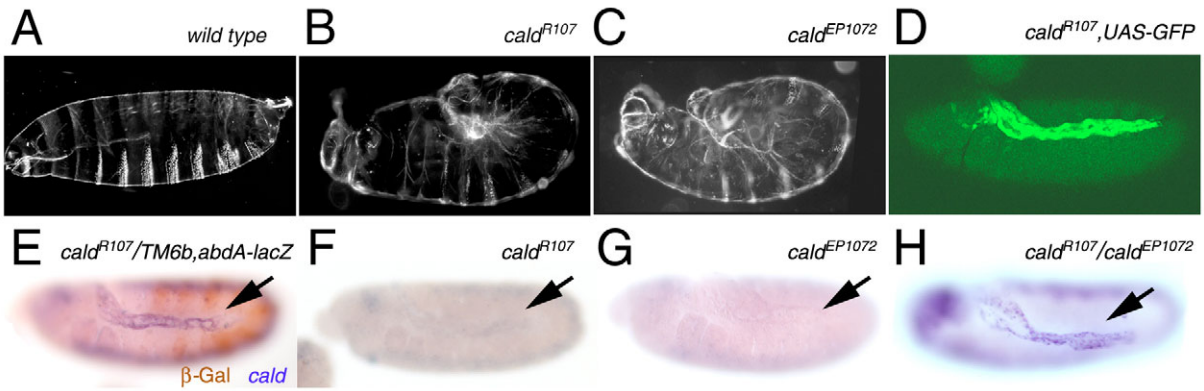

Fig. 2. *calderón* embryonic phenotype. (**A-C**) Lateral view (anterior left, dorsal up) of wild-type (A), *cald*^{R107}/*cald*^{R107} (B), and *cald*^{EP1072}/*cald*^{EP1072} (C) first instar larvae. Mutant embryos exhibit the characteristic U-shaped phenotype due to a defective germ band retraction. (**D**) Lateral view of a *cald*^{R107} embryo driving the expression of GFP in the *calderón* pattern. (**E-H**) Lateral view of embryos showing the distribution of *CG13610* transcripts. Note reduced expression levels in *cald*^{R107} (F) or *cald*^{EP1072} (G) mutant embryos, when compared with heterozygous *cald*^{R107} (E) or *cald*^{R107}/*cald*^{EP1072} (H) embryos. Arrows point to the amnioserosa. Double in situ hybrdization and antibody staining against β-Gal protein (brown in E) was performed to identify homozygous and heterozygous *cald* embryos.

Fortuitously, the lethal excision lines *cald*^{R106} and *cald*^{R107} (but not *cald*^{R165}) leave *GAL4* and the cis-regulatory regions unaffected, so that the mutants express *GAL4* in the normal pattern of *calderón* (Fig. 2D). Interestingly, these two alleles complemented the lethal allele *cald*^{EP1072}, probably as a result of the capacity of *GAL4* expressed in the normal pattern of *cald* (in *cald*^{R106} and *cald*^{R107} P-element insertions) to drive the expression of *CG13610* under the control of the GAL4-binding sites (in the *cald*^{EP1072} insertion, Fig. 2H). It is well known the GAL4/UAS system is cold sensitive, being most effective at 25°C. *cald*^{R106}/*cald*^{EP1072} adult flies did not show any growth defect when raised at 25°C (Fig. 3F,G). When raised at 18°C, flies were smaller (Fig. 3F,G), resembling the growth phenotype of the *cald* viable allele *cald*^{R161}. Taken together, these results indicate that the embryonic phenotype and the growth defects of the *cald* mutants are caused by the absence of *CG13610* expression.

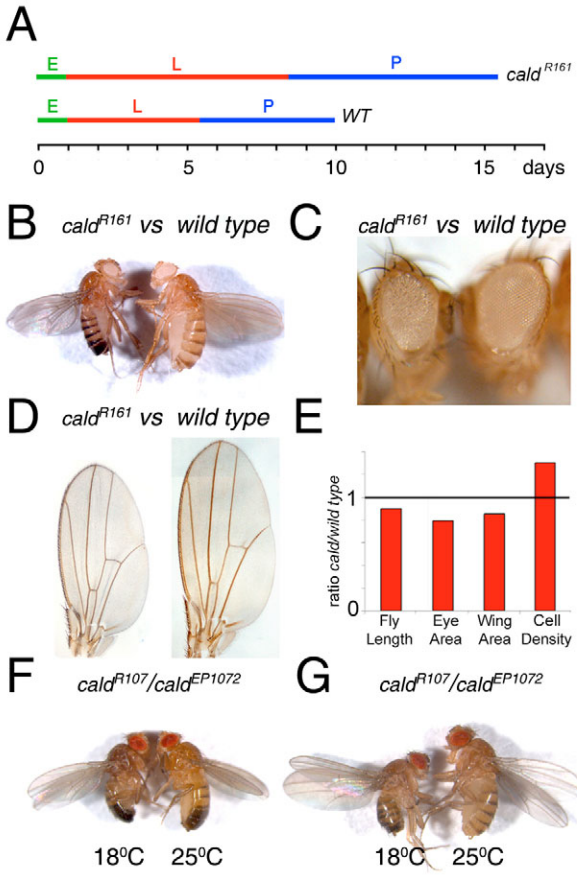

Fig. 3. *calderón* adult phenotype. (**A**) Graph depicting the developmental delay of *cald*^{R161} animals. The length of embryonic (E, green), larval (L, red) and pupal (P, blue) stages is shown for *cald*^{R161} and wild-type animals. (**B**) *cald*^{R161} animals are smaller than wild-type ones. (**C**) *cald*^{R161} and wild-type heads; note the *cald*^{R161} eye is markedly smaller. (**D**) *cald*^{R161} and wild-type wings. Note the *cald*^{R161} wing is smaller than the wild-type one. (**E**) Histogram plotting the size and cell density ratio of *calderón*/wild-type animals. Ratio (fly length): 0.9±0.04; ratio (eye size): 0.8±0.05; ratio (wing size): 0.85±0.04; ratio (cell density): 1.3±0.16. Number of scored flies: n (wt):7; n (cald):9. Number of scored eyes: n (wt):7; n (cald):9. Number of scored wings: n (wt):6; n (cald):6. Number of scored wings for cell density counting: n (wt):7; n (cald):9. (**F**,**G**) *cald*^{R107}/*cald*^{EP1072} male (F) and female (G) animals are smaller than wild-type ones when raised at 18°C, but nearly wild-type at 25°C.

Cells lacking *calderón* show reduced proliferation and are eliminated by cell competition

To study *cald* requirement during imaginal development we induced clones of cells mutant for *cald*. Lethal allele $cald^{R107}$ was used in this analysis. The frequencies and sizes of *cald* mutant clones and their twin clones were similar 24 h after induction (Fig. 4A), but after 48 h *cald* mutant clones contained significantly fewer cells and were recovered at a lower frequency (Fig. 4B). At 72 h after induction, mutant clones were not recovered (Fig. 4C), indicating that *cald* homozygous cells were eliminated from the disc epithelium. Clones expressing a *cald* transgene (Fig. 4D) under the control of the tubulin promoter [using the MARCM technique (Lee and Luo, 1999)] were recovered 72 h after induction, demonstrating that these defects are caused by loss of *cald* activity.

All these results indicate that *cald* mutant cells can perform several rounds of divisions but at a lower rate than control cells. Thus, their elimination might be due to cell competition of slow-dividing cells (Morata and Ripoll, 1975; Moreno et al., 2002). Indeed, $cald^{R107}$ clones show increased activity of the effector caspase drice (Fraser et al., 1997), a cysteine protease that degrades the cellular substrates and causes cell death (Fig. 4E,E′). This apoptosis is associated with the upregulation of *brinker* (Moreno et al., 2002). $cald^{R107}$ clones also exhibit upregulation of the expression of this gene (Fig. 4F,F′).

To circumvent the problem caused by slow proliferation and apoptosis of *cald* mutant cells, and to verify that these cells are lost by cell competition, we used the *Minute* technique (Fig. 5A) (Morata and Ripoll, 1975) to increase their proliferation rate. The *Minute* mutations are defective in ribosomal proteins, and in heterozygous conditions produce a developmental delay caused by their low division rate. *cald Minute*$^+$ clones growing in a *Minute*/+ background lost the retarding *Minute* condition and compensated for the slowdown of proliferation. Under these conditions, *cald Minute*$^+$ clones were recovered (Fig. 5C,E,G). However, they were smaller than wild-type control clones (compare Fig. 5F with G). The size ratio of *calderón*/wild-type clones was 0.13±0.1, and the density ratio was 1.24±0.29. Thus, the average number of cells per clone and the cell size were reduced, indicating that the loss of *cald* activity makes cells grow and proliferate at slower rates.

The *Minute* homozygous condition is cell lethal. Under normal circumstances, *Minute* homozygous cells resulting from mitotic recombination (Fig. 5A) were not recovered 48 h after induction (Fig. 5D). When *cald Minute*$^+$ mutant clones were analyzed, the frequency of recovered *Minute*$^-$ clones was much higher than expected (Fig. 5C,E,G-I). These results indicate that *Minute*$^-$ homozygous clones are eliminated from the disc epithelium as a result of cell competition and either the loss of *cald* activity in neighbouring cells (i.e. the mutant clones), or the cell-autonomous increase in *cald* activity in the *Minute*$^-$ homozygous cells reduces cell competition and allows *Minute*$^-$ cells to survive longer.

The examination of *cald* mutant clones in the wing epithelium and adult cuticle revealed that mutant cells were smaller (Fig. 6). $cald^{R107}$ *Minute*$^+$ cells were smaller than wild-type cells in the wing epithelium (Fig. 6A,B), and differentiated thinner and shorter bristles at the adult wing margin (Fig. 6E,F) and in the notum (Fig. 6C,D). These results indicate that *cald* has a cell-autonomous effect on cell size.

Growth stimulation by the InR pathway requires *calderón*

The *cald* embryonic phenotype and the cell-autonomous effect on the rate of cell division are reminiscent of mutations in components of the InR signalling pathway (Coelho and Leevers, 2000). It is conceivable that *cald* is a new component or target of the InR pathway. In response to ligand binding, the InR phosphorylates the Insulin Receptor Substrate (IRS) proteins (encoded by *chico* in *Drosophila*) (Böhni et al., 1999), thereby activating the class I PI 3-kinase (PI3K), which in turn increases the levels of the second messenger phosphatidylinositol 3,4,5-tryphosphate (PIP_3) at the cell membrane (Fig. 8). The serine threonine protein kinase Akt appears to be the major critical target of PIP_3 signalling in *Drosophila*. Two signalling branches downstream of Akt have been identified. One leads to activation of TOR and S6K through Rheb kinase activity. The *Drosophila Rheb* functions in the InR pathway downstream of Tsc1-Tsc2, and its overexpression causes activation of this pathway, leading to increased cell proliferation (Garami et al., 2003; Zhang et al., 2003). To determine whether *cald* is required for Rheb signalling, we used the MARCM technique to examine the growth properties of clones of cells that lack *cald* and overexpress *Rheb* (Lee and Luo, 1999). *Rheb* overexpression did not induce growth in *cald* mutant cells and these clones were lost 72 h after induction (not shown). We therefore conclude that *cald* functions downstream of or in parallel to Rheb signalling.

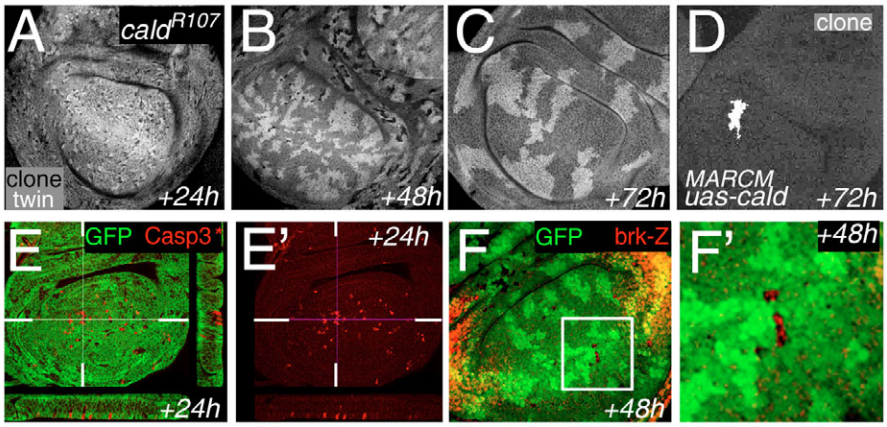

Fig. 4. *calderón* mutant cells are eliminated by cell competition. (**A-C**) Wing discs with $cald^{R107}$ mutant clones marked by the absence of expression of the *lacZ* gene, as visualized with an antibody against the β-Gal protein (grey). Twins were marked by the presence of two copies of *lacZ* (white). Larvae were dissected 24 (A), 48 (B) and 72 (C) h after clone induction. Twins were larger than mutant clones and 72 h after induction *cald* mutant cells disappeared. (**D**) Rescue of $cald^{R107}$ mutant cells by expression of an *UAS-cald* transgene using the MARCM technique. Clones were visualized 72 h after induction by the expression of an *UAS-GFP* transgene (white). (**E**,E′) $cald^{R107}$ mutant clones marked by the absence of the GFP marker (green) and visualized 24 h after induction. Expression of the activated form of the Caspase-3 protein is shown in red. The upper panel shows an XY confocal section of the wing pouch. The right and lower panels show YZ and XZ sections of the same wing discs at the level of the white lines. (**F**,F′) *brinker* (*brk*) expression in *cald* mutant cells. $cald^{R107}$ mutant clones marked by the absence of the GFP marker (green) show an up-regulation of *brk-lacZ* expression (in red).

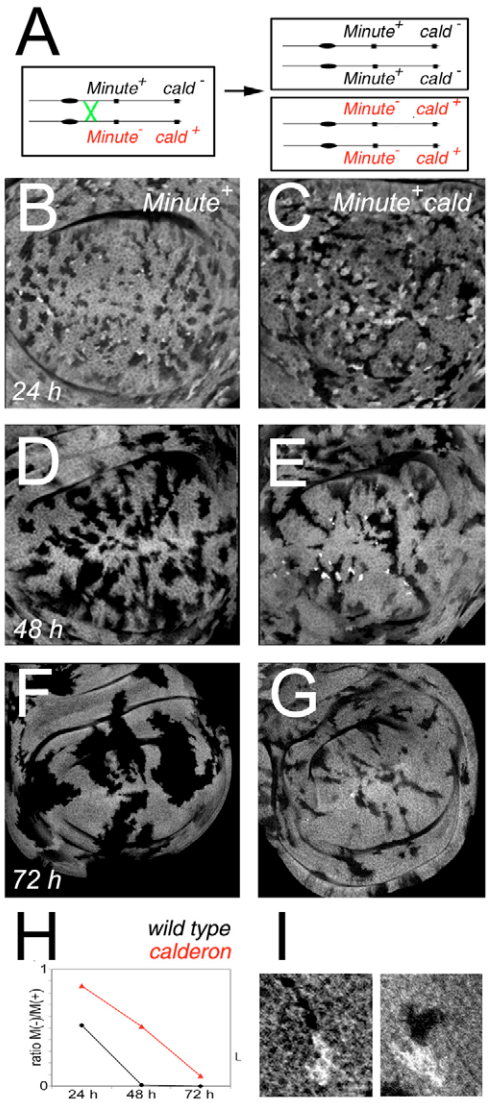

Fig. 5. The role of *calderón* activity in *Minute* mediated cell competition. (**A**) Diagram depicting the induction of *Minute*$^+$ *cald* mutant clones (upper cell) and their *Minute*$^-$ *cald*$^+$ twins (lower cell) after a mitotic recombination event. (**B-G**,**I**) Clones are marked by the absence of the β-Gal marker (grey). Twins are marked by the presence of two copies of the β-Gal marker (white). (B,D,F) *Minute*$^+$ control clones visualized 24 (B), 48 (D) and 72 (F) h after induction. Note all twin *Minute*$^-$ homozygous clones have already disappeared 48 h after induction. (C,E,G,I) *cald Minute*$^+$ clones visualized 24 (C), 48 (E) and 72 (G,I) h after induction. Some twins (*Minute*$^-$ homozygous and wild type for *cald* function) are recovered even 72 h after induction (magnified in I). (**H**) Graph plotting the ratio of *Minute*$^-$/*Minute*$^+$ control clones (in black) and the ratio of *Minute*$^-$/*Minute*$^+$ *cald* mutant clones (in red). 24 h after clone induction: number of *Minute*$^+$ clones: 522; number of *Minute*$^+$ *cald* clones: 253. 48 h after clone induction: number of *Minute*$^+$ clones: 507; number of *Minute*$^+$ *cald* clones: 187. 72 h after clone induction: number of *Minute*$^+$ clones: 58; number of *Minute*$^+$ *cald* clones: 81.

A major effector of Rheb function is S6K (Stocker et al., 2003). Genetic evidence has established that insulin exerts many of its cellular effects by triggering the activation of S6K (p70 ribosomal S6 kinase). Full activation of dS6K requires two distinct signals, one in response to growth factors and another from a nutrient sensing pathway, and thus provides a mechanism whereby individual cells can coordinate their response to growth factors with nutrient availability (Zhang et al., 2003). To determine whether *cald* is involved in nutrient sensing, we examined the growth properties of clones of cells that lack *cald* and overexpress dS6K. As with Rheb, cells overexpressing dS6K but lacking *cald* activity were lost by 72 h after clone induction (not shown). We conclude that *cald* is not involved in nutrient sensing and is epistatic to *S6K*. Therefore, *cald* functions downstream of or in parallel to S6K signalling.

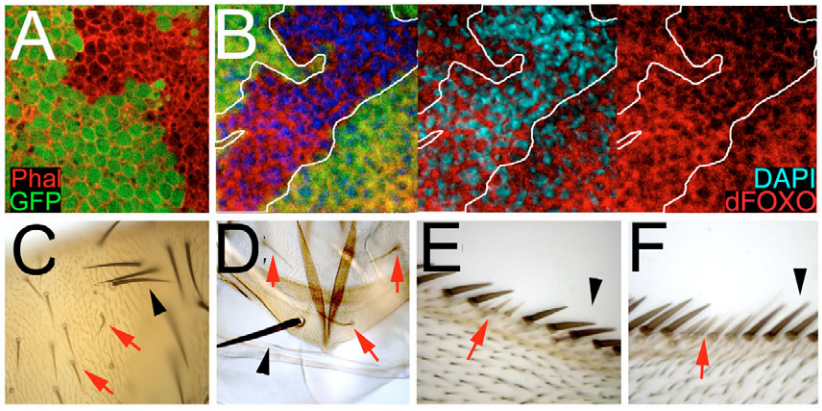

Fig. 6. *calderón* clonal phenotypes. (**A**,**B**) *cald* mutant cells are small in imaginal discs. *Minute*$^+$ *cald*^{R107} mutant clones marked by the absence of the GFP marker (green) in the wing imaginal disc. Cell membranes are delineated by Phaloidin (red in A) and cell nuclei are labelled by DAPI (blue in B). dFOXO (red in B) remains cytoplasmic in *cald* clones.The white trace outlines the mutant clone in B. (**C-F**) *cald* mutant cells are small in the adult. Clones of *Minute*$^+$ *cald* mutant cells marked by the absence of the *P(yellow*$^+$*)* rescue construct in the notum (C,D), and in the wing margin (E,F). Each hair-like structure is a trichome emanating from a single epithelial cell. Note the reduced size and increased density of *cald* cells (red arrow) compared with surrounding *yellow*$^+$ ones (black arrowhead).

A second pathway downstream of Akt has been identified. The Forkhead-related transcription factor dFOXO is phosphorylated by Akt upon insulin signalling, leading to cytoplasmatic retention and inhibition of its transcriptional activity. Upon reduced insulin signalling, dFOXO becomes dephosphorylated and accumulates in the nucleus, where it regulates the transcription of a number of target genes, thereby leading to cell death or cell cycle arrest (Junger et al., 2003; Kramer et al., 2003; Puig et al., 2003). To determine whether *cald* is required for dFOXO inhibition, we examined the subcellular location of dFOXO in clones of *cald* mutant cells, and found that dFOXO remains cytoplasmic in these clones (Fig. 6B). We conclude that Akt inhibits dFOXO in the absence of *cald* function. These results indicate that *cald* is not required for dFOXO inhibition.

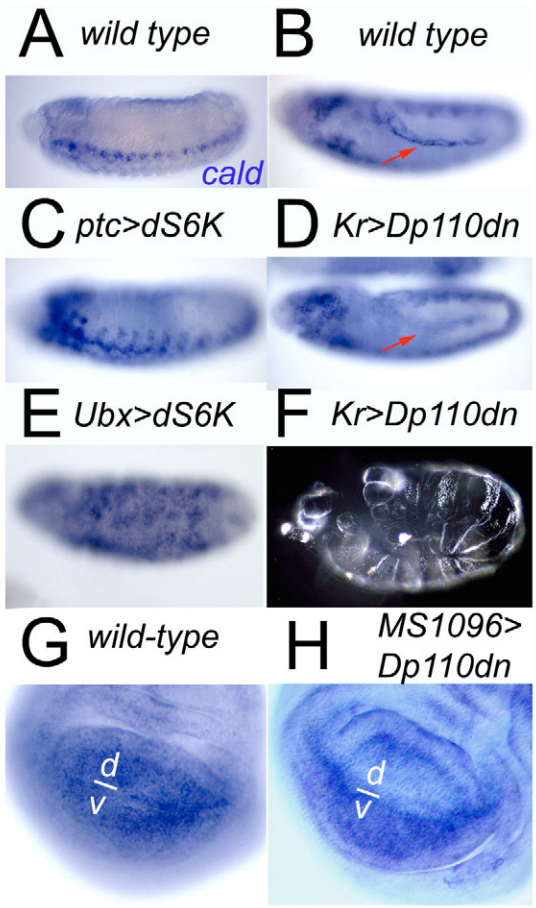

Fig. 7. *calderón* expression is regulated by the Insulin pathway. (**A-E**) Lateral view (anterior left, dorsal up) of embryos showing the distribution of *cald* transcripts in various genetic backgrounds. (A,C,E) Activation of the InR pathway up-regulates *cald* expression. Stage 13 embryos showing *cald* transcripts in wild-type (A), *ptc-Gal4:UAS-dS6K* (C) and *Ubx-Gal4:UAS-dS6K* (E) backgrounds. At this stage, wild-type embryos show *cald* expression only in amnioserosa and a group of cells of the CNS. Activation of InR pathway in ectodermal cells in *ptc* (C) and *Ubx* (E) domains up-regulates *cald* expression in the ectoderm. (B,D) Down-regulation of the InR pathway eliminates *cald* expression. Stage 11 embryos showing *cald* transcripts in *wt* (B) and *Kr-Gal4:UAS- PI3K92E-Dp110^{DN}* (D) backgrounds. Note reduced expression of *cald* in amnioserosa cells in D (red arrow). (**F**) Down-regulation of InR pathway in amnioserosa cells phenocopies *cald* mutants. Lateral view of *Kr-Gal4:UAS- PI3K92E-Dp110 ^{DN}* first instar larva. These larvae exhibit the characteristic U-shaped phenotype of *cald* mutants (compare Fig. 2B with C). (**G**,**H**) Third instar wing discs showing *cald* transcripts in wild-type (G) and *MS1096-Gal4:UAS-PI3K92E-Dp110^{DN}* (H) backgrounds. *MS1096-Gal4* is expressed at higher levels in the dorsal compartment (d) of the wing pouch. The boundary between dorsal (d) and ventral (v) compartment is shown.

InR pathway regulates *calderón* expression

PI3K and TOR-mediated signals exert some of their growth effects at the transcriptional level (reviewed in Neufeld, 2003). TOR controls expression of a broad group of genes with roles in protein, lipid and nucleic acid metabolism (Beck and Hall, 1999; Cardenas et al., 1999). In addition, both TOR and PI3K affect the expression and activity of the C/EBP family of transcriptional regulators, which regulates the expression of a number of genes in response to nutrients (Entingh et al., 2001; Roesler, 2001). Thus, given that the InR signalling pathway controls the expression of a diverse spectrum of metabolism-related genes, we examined whether this pathway activates *cald* transcription. To address this issue, *cald* expression was first analyzed in the embryo following expression of either *S6K* or a dominant-negative form of the *Drosophila* PI3K (*PI3K92E-Dp110^{D954A}*). Expression of *S6K* in the *patched* or *Ubx* domains induced ectopic *cald* expression (Fig. 7C,E, compare with 7A). When a dominant-negative version of *PI3K92E-Dp110 (PI3K92E-Dp110^{D954A}*) was expressed in amnioserosa cells under the control of the *Kr-GAL4* driver, *cald* expression was reduced in these cells (compare Fig. 7B with D, red arrows). Furthermore, these embryos did not retract the germ band (Fig. 7F), as expected for an embryo that lacks *cald* expression in the amnioserosa (Fig. 2B,C). When *PI3K92E-Dp110^{D954A}* was expressed in the dorsal side of the wing imaginal disc under the control of the *MS1096-GAL4* driver, *cald* expression was reduced (compare Fig. 7G with H). Expression of *S6K* in the *patched* domain did not increase *cald* expression in the wing disc, suggesting that the expression levels of this gene are saturated in imaginal cells (data not shown). Consistent with this, over-expression of *cald* in clones of cells did not cause any overt phenotype in terms of growth, cell size or cell competition (data not shown). Taken together, the data indicate that *cald* expression is regulated by the InR pathway in the embryo and in imaginal cells.

Concluding remarks

Genetic studies have revealed a key role for InR signalling in coordinating growth and other nutrition-regulated functions in flies. Although the distinct elements of this pathway have been well described, the downstream elements responsible for this task remain to be fully elucitated. *calderón*, a gene encoding for an Organic Cation Transporter, is regulated at a transcriptional level by the PI3-kinase/TOR pathway (Fig. 8). *cald* mutant flies are smaller than wild-type ones and show a developmental delay. Clones of cells mutant for *cald* divide more slowly, are smaller than wild-type cells and are eliminated by cell competition. However, when *cald* clones have a proliferative advantage in a *Minute* heterozygous background, they are not eliminated and are able to differentiate normal adult structures, although they are smaller than wild-type ones. Since *cald* vertebrate orthologs are involved in carrying organic substrates across the plasma membrane (Grundemann et al., 2005), we propose that reduced *cald* activity in proliferating cells impairs competition for organic substrates available in the extracellular media. This impairment may again represent (Moreno et al., 2002) another mechanism by which weaker cells are removed from a growing population, and might serve to regulate cell number and optimise tissue fitness and hence organ function.

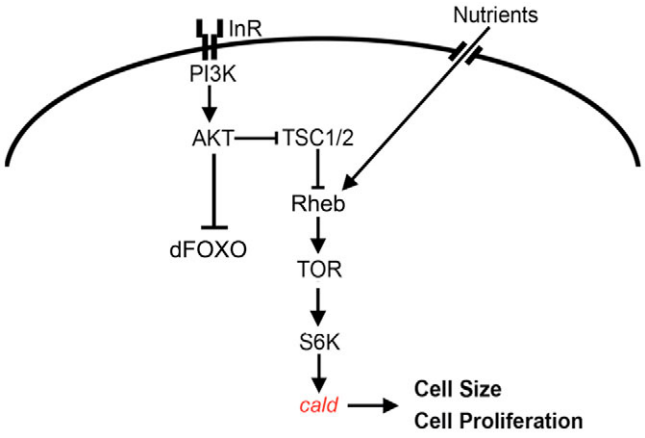

Fig. 8. Mode of action of Calderón. Proposed model illustrating the role of *cald* in *Drosophila* growth. Genetic and/or biochemical relationships are depicted as arrows to indicate positive regulators or as bars to represent negative regulators of targets. The TOR and InR pathways integrate the nutritional information and exert a control on cell growth, in part, regulating *cald* expression. Cald activity is required for the control of growth: cell size and proliferation.

cald activity is required for PI3-kinase/TOR function in inducing growth: up-regulation of this pathway in a *cald* mutant background does not affect growth. Furthermore, *cald* expression is dependent on PI3-kinase activity, as embryos overexpressing S6K show increased *cald* levels, whereas expression of a dominant negative form of PI3K (*PI3K92E-Dp110*^{D954A}) reduces them. Thus, we propose that *cald* responds to InR activity levels and that it is required, in a cell-autonomous way, for cell growth and proliferation. We hypothesize that the growth of imaginal cells is then controlled by two distinct, but coordinated, nutrient-sensing mechanisms. A cell autonomous mechanism (e.g. *cald*) may directly detect nutrient levels in the haemolympha, thus changing the response of cells to insulin. The fat body, functioning as a nutrient sensor of the media, may then regulate the growth of the whole organism, perhaps by modulating the levels of membrane transporters, like Cald, that carry nutrients across the membrane.

We thank B. Edgar, P. Leopold, T. Neufeld, O. Puig, E. Hafen and the *Drosophila* Bloomington Stock Center for reagents. We also thank A. Pérez-Garijo, C. Estella, F. A. Martín, T. Yates, two anonymous reviewers and members of our laboratories for comments on the manuscript, and R. González and A. Cantarero for technical help. H.H. is a recipient of a Juan de la Cierva postdoctoral contract. Research in the M.M.'s laboratory is funded by a grant from the Dirección General de Investigación Científica y Técnica (BFU2004-00167/BMC) and by EU research contract LSHM-CP-2003-503330 (APOPIS). Work in G.M.'s laboratory is funded by a grant from the Dirección General de Investigación Científica y Técnica (BMC2002-01959).

References

Azpiazu, N. and Frasch, M. (1993). tinman and bagpipe: two homeo box genes that determine cell fates in the dorsal mesoderm of Drosophila. *Genes Dev.* **7**, 1325-1340.
Beck, T. and Hall, M. N. (1999). The TOR signalling pathway controls nuclear localization of nutrient-regulated transcription factors. *Nature* **402**, 689-692.
Böhni, R., Riesgo-Escovar, J., Oldham, S., Brogiolo, W., Stocker, H., Andruss, B. F., Beckingham, K. and Hafen, E. (1999). Autonomous control of cell and organ size by CHICO, a Drosophila homolog of vertebrate IRS1-4. *Cell* **97**, 865-875.
Brand, A. H. and Perrimon, N. (1993). Targeted gene expression as a means of altering cell fates and generating dominant phenotypes. *Development* **118**, 401-415.
Bulter, A. A. and Le Roith, D. (2001). Control of growth by the somatropic axis: growth hormone and the insulin-like growth factors have related and independent roles. *Annu. Rev. Physiol.* **63**, 141-164.
Calleja, M., Moreno, E., Pelaz, S. and Morata, G. (1996). Visualization of gene expression in living adult Drosophila. *Science* **274**, 252-255.
Cardenas, M. E., Cutler, N. S., Lorenz, M. C., Di Como, C. J. and Heitman, J. (1999). The TOR signaling cascade regulates gene expression in response to nutrients. *Genes Dev.* **13**, 3271-3279.
Castelli-Gair, J., Greig, S., Micklem, G. and Akam, M. (1994). Dissecting the temporal requirements for homeotic gene function. *Development* **120**, 1983-1995.
Coelho, C. M. and Leevers, S. J. (2000). Do growth and cell division rates determine cell size in multicellular organisms? *J. Cell Sci.* **113**, 2927-2934.
Conlon, I. and Raff, M. (1999). Size control in animal development. *Cell* **96**, 235-244.
Efstratiadis, A. (1998). Genetics of mouse growth. *Int. J. Dev. Biol.* **42**, 955-976.
Entingh, A. J., Law, B. K. and Moses, H. L. (2001). Induction of the C/EBP homologous protein (CHOP) by amino acid deprivation requires insulin-like growth factor I, phosphatidylinositol 3-kinase, and mammalian target of rapamycin signaling. *Endocrinology* **142**, 221-228.
Fernandez, R., Tabarini, D., Azpiazu, N., Frasch, M. and Schlessinger, J. (1995). The *Drosophila* insulin receptor homolog: a gene essential for embryonic development encodes two receptor isoforms with different signaling potential. *EMBO J.* **14**, 3373-3384.
Frank, L. H. and Rushlow, C. (1996). A group of genes required for maintenance of the amnioserosa tissue in Drosophila. *Development* **122**, 1343-1352.
Fraser, A. G., McCarthy, N. J. and Evan, G. I. (1997). drICE is an essential caspase required for apoptotic activity in Drosophila cells. *EMBO J.* **16**, 6192-6199.
Garami, A., Zwartkruis, F. J., Nobukuni, T., Joaquin, M., Roccio, M., Stocker, H., Kozma, S. C., Hafen, E., Bos, J. L. and Thomas, G. (2003). Insulin activation of Rheb, a mediator of mTOR/S6K/4E-BP signaling, is inhibited by TSC1 and 2. *Mol. Cell* **11**, 1457-1466.
Goberdhan, D. C. and Wilson, C. (2003). The functions of insulin signaling: size isn't everything, even in Drosophila. *Differentiation* **71**, 375-397.
Grundemann, D., Harlfinger, S., Golz, S., Geerts, A., Lazar, A., Berkels, R., Jung, N., Rubbert, A. and Schomig, E. (2005). Discovery of the ergothioneine transporter. *Proc. Natl. Acad. Sci. USA* **102**, 5256-5261.
Hay, B. A., Wassarman, D. A. and Rubin, G. M. (1995). Drosophila homologs of baculovirus inhibitor of apoptosis proteins function to block cell death. *Cell* **83**, 1253-1262.
Herranz, H. and Morata, G. (2001). The functions of pannier during Drosophila embryogenesis. *Development* **128**, 4837-4846.
Jazwinska, A., Kirov, N., Wieschaus, E., Roth, S. and Rushlow, C. (1999). The Drosophila gene brinker reveals a novel mechanism of Dpp target gene regulation. *Cell* **96**, 563-573.
Junger, M. A., Rintelen, F., Stocker, H., Wasserman, J. D., Vegh, M., Radimerski, T., Greenberg, M. E. and Hafen, E. (2003). The Drosophila forkhead transcription factor FOXO mediates the reduction in cell number associated with reduced insulin signaling. *J. Biol.* **2**, 20.
Kramer, J. M., Davidge, J. T., Lockyer, J. M. and Staveley, B. E. (2003). Expression of Drosophila FOXO regulates growth and can phenocopy starvation. *BMC Dev. Biol.* **3**, 5.
Lee, T. and Luo, L. (1999). Mosaic analysis with a repressible cell marker for studies of gene function in neuronal morphogenesis. *Neuron* **22**, 451-461.
Leevers, S. J., Weinkove, D., MacDougall, L. K., Hafen, E. and Waterfield, M. D. (1996). The *Drosophila* phosphoinositide 3-kinase Dp110 promotes cell growth. *EMBO J.***15**, 6584-6594.
Milan, M., Diaz-Benjumea, F. J. and Cohen, S. M. (1998). Beadex encodes an LMO protein that regulates Apterous LIM-homeodomain activity in Drosophila wing development: a model for LMO oncogene function. *Genes Dev.* **12**, 2912-2920.
Morata, G. and Ripoll, P. (1975). Minutes: mutants of Drosophila autonomously affecting cell division rate. *Dev. Biol.* **42**, 211-221.
Moreno, E., Basler, K. and Morata, G. (2002). Cells compete for decapentaplegic survival factor to prevent apoptosis in Drosophila wing development. *Nature* **416**, 755-759.
Neufeld, T. P. (2003). Body building: regulation of shape and size by PI3K/TOR signaling during development. *Mech. Dev.* **120**, 1283-1296.
Peltekova, V. D., Wintle, R. F., Rubin, L. A., Amos, C. I., Huang, Q., Gu, X., Newman, B., Van Oene, M., Cescon, D., Greenberg, G. et al. (2004). Functional variants of OCTN cation transporter genes are associated with Crohn disease. *Nat. Genet.* **36**, 471-475.
Puig, O., Marr, M. T., Ruhf, M. L. and Tjian, R. (2003). Control of cell number by Drosophila FOXO: downstream and feedback regulation of the insulin receptor pathway. *Genes Dev.* **17**, 2006-2020.
Roesler, W. J. (2001). The role of C/EBP in nutrient and hormonal regulation of gene expression. *Annu. Rev. Nutr.* **21**, 141-165.
Rulifson, E. J., Kim, S. K. and Nusse, R. (2002). Ablation of insulin-producing neurons in flies: growth and diabetic phenotypes. *Science* **296**, 1118-1120.
Saucedo, L. J., Gao, X., Chiarelli, D. A., Li, L., Pan, D. and Edgar, B. A. (2003).

Rheb promotes cell growth as a component of the insulin/TOR signalling network. *Nat. Cell Biol.* **5**, 566-571.
Shioi, T., Kang, P. M., Douglas, P. S., Hampe, J., Yballe, C. M., Lawitts, J., Cantley, L. C. and Izumo, S. (2000). The conserved phosphoinositide 3-kinase pathway determines heart size in mice. *EMBO J.* **19**, 2537-2548.
Shioi, T., McMullen, J. R., Kang, P. M., Douglas, P. S., Obata, T., Franke, T. F., Cantley, L. C. and Izumo, S. (2002). Akt/protein kinase B promotes organ growth in transgenic mice. *Mol. Cell. Biol.* **22**, 2799-2809.
Stern, D. L. and Emlen, D. J. (1999). The developmental basis for allometry in insects. *Development* **126**, 1091-1101.
Stocker, H. and Hafen, E. (2000). Genetic control of cell size. *Curr. Opin. Genet. Dev.* **10**, 529-535.
Stocker, H., Radimerski, T., Schindelholz, B., Wittwer, F., Belawat, P., Daram, P., Breuer, S., Thomas, G. and Hafen, E. (2003). Rheb is an essential regulator of S6K in controlling cell growth in Drosophila. *Nat. Cell Biol.* **5**, 559-565.
Tabata, T., Schwartz, C., Gustavson, E., Ali, Z. and Kornberg, T. B. (1995). Creating a Drosophila wing de novo: the role of *engrailed* and the compartment border hypothesis. *Development* **121**, 3359-3369.
Tautz, D. and Pfeifle, C. (1989). A non-radioactive in situ hybridization method for the localization of specific RNAs in Drosophila embryos reveals translational control of the segmentation gene hunchback. *Chromosoma* **98**, 81-85.
Tokuhiro, S., Yamada, R., Chang, X., Suzuki, A., Kochi, Y., Sawada, T., Suzuki, M., Nagasaki, M., Ohtsuki, M., Ono, M. et al. (2003). An intronic SNP in a RUNX1 binding site of SLC22A4, encoding an organic cation transporter, is associated with rheumatoid arthritis. *Nat. Genet.* **35**, 341-348.
Wilder, E. L. and Perrimon, N. (1995). Dual functions of *wingless* in the *Drosophila* leg imaginal disc. *Development* **121**, 477-488.
Xu, T. and Rubin, G. M. (1993). Analysis of genetic mosaics in developing and adult *Drosophila* tissues. *Development* **117**, 1223-1237.
Zhang, Y., Gao, X., Saucedo, L. J., Ru, B., Edgar, B. A. and Pan, D. (2003). Rheb is a direct target of the tuberous sclerosis tumour suppressor proteins. *Nat. Cell Biol.* **5**, 578-581.